The Characteristics of Microwave Melting of Frozen Packed Beds Using a Rectangular Waveguide

Phadungsak Ratanadecho, Kazuo Aoki, and Masatoshi Akahori

***Abstract*—The melting of frozen packed beds by a microwave with a rectangular waveguide has been investigated numerically and experimentally. It was performed for the two different layers, which consist of frozen and unfrozen layers. This paper focuses on the prediction of the temperature field, as well as the microwave energy absorbed, and the melting front within the layered packed beds. Based on the combined model of the Maxwell and heat transport equations, the results show that the direction of melting against the incident microwave strongly depends on the structural layered packed beds because of the difference in the dielectric properties between water and ice.**

***Index Terms*—FDTD method, layered packed beds, microwave melting, moving boundary, rectangular waveguide.**

NOMENCLATURE

a	Thermal diffusivity (m^2/s).
C_p	Specific heat capacity (J/kg · K).
E	Electric field intensity (V/m).
f	Frequency of incident wave (Hz).
H	Magnetic field intensity (A/m).
L	Latent heat (J/kg).
Q	Microwave energy absorbed term (W/m^3).
T	Temperature (C).
t	Time (s).
$\tan\delta$	Loss tangent coefficient (-).
x, y, z	Cartesian coordinates (-).

Greek letters

ε	Permittivity (F/m).
μ	Magnetic permeability (H/m).
υ	Velocity of microwave (m/s).
σ	Electric conductivity (S/m).
ω	Angular frequency (rad/s).
λ	Effective thermal conductivity (W/mK).

Subscripts

0	Free space.
a	Air.
j	Layer number.
l	Liquid.
r	Relative.
s	Solid.

Manuscript received December 17, 2000. This work was supported by the Japanese Ministry of Education under a science research grant.

The authors are with the Mechanical Engineering Department, Nagaoka University of Technology, Niigata 940-2188, Japan (e-mail: phadu@blue.nagaokaut.ac.jp).

Publisher Item Identifier S 0018-9480(02)05204-3.

I. INTRODUCTION

A STUDY OF the melting process in material expose to a microwave was studied by Pangrle *et al.* [1], in which a one-dimensional model was developed for microwave melting of cylinders. Later, Zeng *et al.* [2] carried out two-dimensional microwave melting in cylinders and their model predictions were compared with experimental data. In a recent paper, Basak *et al.* [3] carried out microwave melting studies with a fixed grid-based effective heat-capacity method coupled with Maxwell's equations.

Other studies of microwave energy applications have appeared in the recent literature (e.g., Torres *et al.* [4], Ratanadecho *et al.* [5], Feher *et al.* [6], Aoki *et al.* [7], and Ratanadecho *et al.* [8]).

Considering the microwave melting process, most previous work used Lambert's law, where the microwave energy absorbed decays exponentially into the sample. However, this assumption is only valid for the large-dimensions sample. For the small sample, the spatial variations of the electromagnetic field as well as microwave energy absorbed within the sample must be obtained by a complete solution of the unsteady Maxwell's equations [8]. Generally, when the boundaries of the physical domain move with time (moving boundary and phase change problems), the melting process in a frozen packed bed is complicated due to the variety of melting conditions. In the past, the melting front in the sample was approximated using a one-dimensional coordinate system. None of the studies modeled the microwave melting process using a general curvilinear coordinate system for calculations of the melting front.

Due to the limited amount of theoretical and experimental work on the microwave melting process, the various effects are not fully understood and a number of critical issues remain unresolved. These effects of the reflection rate of microwave, the degree of incident wave penetrated into the sample as well as the microwave energy absorbed during the microwave melting process have not been studied systematically.

This paper reports a comparison of simulation results based on a two-dimensional model with experimental measurements in which the microwave of the TE_{10} mode operating at a frequency of 2.45 GHz is performed. Furthermore, in order to calculate the melting front during the microwave melting process, a general curvilinear coordinate system is employed.

II. ANALYSIS OF MICROWAVE MELTING USING A RECTANGULAR WAVEGUIDE

A. Analysis of Electromagnetic Field

Fig. 1 shows the physical model for microwave melting of layered packed beds using a rectangular waveguide.

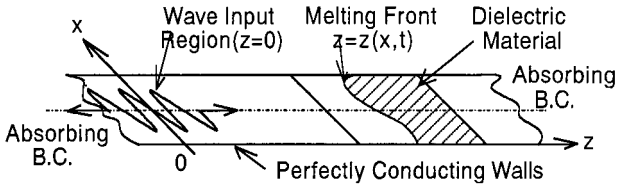

Fig. 1. Physical model.

1) Assumptions: The proposed model is based on the following assumptions.

- Since the microwave field in the TE_{10} mode has no variation of field in the direction between the broad faces, a two-dimensional model over the x-z plane is applicable to the analysis of the electromagnetic field inside a rectangular waveguide [6].
- The absorption of microwave energy by the cavity (including air) in the rectangular waveguide is negligible.
- The walls of a rectangular waveguide are perfect conductors.
- The effect of the sample container on the electromagnetic field can be neglected.

2) Basic Equations: The basic equations for the electromagnetic field are based on the well-known Maxwell relations. For the microwave of the TE_{10} mode [8], the governing equations can be written in term of the component notations of electric- and magnetic-field intensities

$$\begin{aligned} \frac{\partial E_y}{\partial z} &= \mu \frac{\partial H_x}{\partial t} \\ \frac{\partial E_y}{\partial x} &= -\mu \frac{\partial H_z}{\partial t} \\ -\left(\frac{\partial H_z}{\partial x} - \frac{\partial H_x}{\partial z}\right) &= \sigma E_y + \varepsilon \frac{\partial E_y}{\partial t} \end{aligned} \tag{1}$$

$$\begin{aligned} \varepsilon &= \varepsilon_0 \varepsilon_r \\ \mu &= \mu_0 \mu_r \\ \sigma &= 2\pi f \varepsilon \tan\delta \end{aligned} \tag{2}$$

where the dielectric properties of components are assumed to be varied with temperature during the heating process [9].

3) Boundary Conditions: Corresponding to the physical model shown in Fig. 1, boundary conditions can be given as follows.

- *Perfectly conducting boundaries*: Boundary conditions on the inner wall surface of a rectangular waveguide are given by using Faraday's law and Gauss' theorem

$$E_t = 0 \quad H_n = 0 \tag{3}$$

  where subscripts t and n denote the components of tangential and normal directions, respectively.
- *Continuity boundary condition*: Boundary conditions along the interface between different materials, e.g., between the air and dielectric material surface, are given by using Ampere's law and Gauss theorem

$$E_t = E_t' \quad H_t = H_t' \quad D_n = D_n' \quad B_n = B_n' \tag{4}$$

  where D is the electric flux density and B is the magnetic induction. The superscript $'$ denotes one of the different materials.
- *Absorbing boundary condition*: At both ends of the rectangular waveguide, the first-order absorbing condition proposed by Mur [10] is applied as follows:

$$\frac{\partial E_y}{\partial t} = \pm \upsilon \frac{\partial E_y}{\partial z}. \tag{5}$$

  Here, the symbol $\pm$ represents forward or backward waves and υ is the phase velocity of microwave.
- *Oscillation of electric- and magnetic-field intensities by the magnetron*: Incident wave due to the magnetron is given by the following:

$$\begin{aligned} E_y &= E_{y\,\mathrm{in}} \sin\left(\frac{\pi x}{L_x}\right) \sin(2\pi f t) \\ H_x &= \frac{E_{y\,\mathrm{in}}}{Z_H} \sin\left(\frac{\pi x}{L_x}\right) \sin(2\pi f t) \end{aligned} \tag{6}$$

  where $E_{y\,\mathrm{in}}$ is the input value of the electric-field intensity, L_x is the length of the rectangular waveguide in x-direction, and Z_H is the wave impedance.

B. Analysis of Heat Transport

The temperature of the sample exposed to incident wave (Fig. 1) is obtained by solving the conventional heat transport equation with the microwave energy absorbed included as a local electromagnetic heat generation term.

1) Assumptions: In order to analyze the process of heat transport due to microwave melting of layered packed beds, we introduce the following assumptions.

- Corresponding to the electromagnetic field, the temperature field also can be assumed to be a two-dimensional plane (x-z plane).
- The surroundings of layered packed beds are insulated.
- The effect of the container on the temperature field can be neglected.
- The effect of the natural convection in layered packed beds can be neglected.
- The local thermodynamic equilibrium is assumed.
- In this study, in a macroscopic sense, the pore structure within the layered packed beds is assumed to be homogeneous and isotropic.

Therefore, the heating model for a homogeneous and isotropic material is used in the current analysis.

2) Basic Equations: The governing energy equation describing the temperature rise in the layered packed beds is the time-dependent heat diffusion equation

$$\frac{\partial T_j}{\partial t} = a\left(\frac{\partial^2 T_j}{\partial x^2} + \frac{\partial^2 T_j}{\partial z^2}\right) + \frac{Q_j}{\rho \cdot C_p}\left(\frac{\partial T_j}{\partial z}\right)\frac{dz}{dt} \tag{7}$$

$$Q_j = 2\pi f \varepsilon_0 \varepsilon_r \tan\delta E_y^2 \tag{8}$$

where a is the thermal diffusivity and Q is the microwave energy absorbed term.

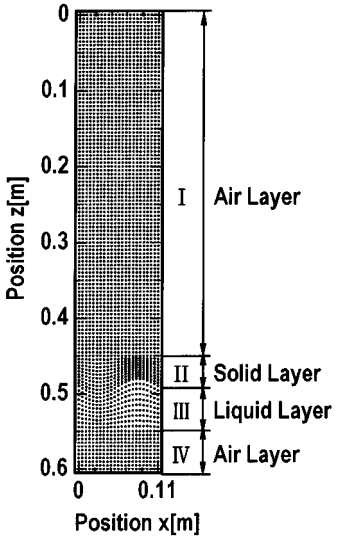

Fig. 2. Typical mesh for the rectangular-waveguide configuration.

3) Boundary Conditions:

- *Adiabatic condition*: Assuming that the surroundings of layered packed beds are insulated

$$\frac{\partial T}{\partial n} = 0 \tag{9}$$

- *Moving front boundary condition*: The moving boundary between the unfrozen layer and frozen layer is described by the Stefan equation

$$\left(\lambda_s \frac{\partial T_s}{\partial z} - q_{\mathrm{Bou}} \Delta z_{\mathrm{Bou}} - \lambda_l \frac{\partial T_l}{\partial z}\right)\left[1 + \left(\frac{\partial z_{\mathrm{Bou}}}{\partial x}\right)^2\right] = \rho_s L_s S_s \frac{\partial z_{\mathrm{Bou}}}{\partial t} \tag{10}$$

where subscript Bou denotes the solid-liquid front.

C. Mesh Construction and Coordinate Transformation

For the construction itself of a coordinate mesh around even the rectangular waveguide as well as the layered packed beds, the method of constructing a two-dimensional boundary-conforming grid for a rectangular waveguide configuration is a direct algebraic approach based on the concept of transfinite or multivariate interpolation [11]. From this concept, the physical domain (Fig. 2) can be divided into the following four layers:

1) air layer (regions I and IV);
2) solid layer (region II);
3) liquid layer (region III).

The boundary between the solid and liquid layers for a melting front is described by the Stefan equation [see (10)]. Furthermore, during the boundaries of the physical domain move with time, it is convenient to introduce a general curvilinear coordinate system as follows:

$$x = x(\xi, \eta) \quad z = z(\xi, \eta)$$

or

$$\xi = \xi(x, z) \quad \eta = \eta(x, z). \tag{11}$$

The moving boundaries are immobilized in the dimensionless (ξ, η) coordinate for all times. With the details omitted, the transformation of (1) and (5) and also (7) and (10) are then defined as

$$\frac{1}{J}\left(x_\xi \frac{\partial E_y}{\partial \eta}\right) = \mu \frac{\partial H_x}{\partial t} \tag{12}$$

$$-\frac{1}{J}\left(z_\eta \frac{\partial E_y}{\partial \xi}\right) - z_\xi \frac{\partial E_y}{\partial \eta} = -\mu \frac{\partial H_z}{\partial t} \tag{13}$$

$$-\frac{1}{J}\left\{\left(z_\eta \frac{\partial H_z}{\partial \xi} - z_\xi \frac{\partial H_z}{\partial \eta}\right) - \left(x_\xi \frac{\partial H_x}{\partial \eta}\right)\right\} = \sigma E_y + \varepsilon \frac{\partial E_y}{\partial t} \tag{14}$$

$$\frac{\partial E_y}{\partial t} = \upsilon \frac{1}{J}\left(x_\xi \frac{\partial E_y}{\partial \eta}\right) \tag{15}$$

$$\begin{aligned}\frac{\partial T_j}{\partial t} = {} & \frac{a}{J^2}\left(\alpha \frac{\partial^2 T_j}{\partial \xi^2} - 2\beta \frac{\partial^2 T_j}{\partial \xi \partial \eta} + \gamma \frac{\partial^2 T_j}{\partial \eta^2}\right) \\ & + \frac{a}{J^3}\left[\left(\alpha \frac{\partial^2 x}{\partial \xi^2}\right)\left(z_\xi \frac{\partial T_j}{\partial \eta} - z_\eta \frac{\partial T_j}{\partial \xi}\right) + \alpha \frac{\partial^2 z}{\partial \xi^2} \right. \\ & \left. -2\beta \frac{\partial^2 z}{\partial \xi \partial \eta} + \gamma \frac{\partial^2 z}{\partial \eta^2}\left(-x_\xi \frac{\partial T_j}{\partial \eta}\right)\right] \\ & + \frac{Q_j}{\rho \cdot C_p} + \frac{1}{J}\left(x_\xi \frac{\partial T_j}{\partial \eta}\right)\frac{dz}{dt} \\ & \cdot \left\{\lambda_s \frac{1}{J}\left(x_\xi \frac{\partial T_s}{\partial \eta}\right) - q_{\mathrm{Bou}} \Delta z_{\mathrm{Bou}} - \lambda_l \frac{1}{J}\left(x_\xi \frac{\partial T_l}{\partial \eta}\right)\right\} \\ & \cdot \left\{1 + \left(\frac{1}{J}\left[z_\eta \frac{\partial z_{\mathrm{Bou}}}{\partial \xi} - z_\xi \frac{\partial z_{\mathrm{Bou}}}{\partial \eta}\right]\right)^2\right\} \\ = {} & \rho_s L_s S_s \frac{\partial z_{\mathrm{Bou}}}{\partial t}\end{aligned} \tag{16, 17}$$

where

$$\begin{aligned} J &= x_\xi \cdot z_\eta - x_\eta \cdot z_\xi \\ \alpha &= x_\eta^2 + z_\eta^2 \\ \beta &= x_\xi \cdot x_\eta + z_\xi \cdot z_\eta \\ \gamma &= x_\xi^2 + z_\xi^2 \end{aligned} \tag{18}$$

where x_ξ, x_η, z_ξ, and z_η denote partial derivatives, J is the Jacobian, β, α, γ are the geometric factors, and η, ξ are the transformed coordinates.

III. Numerical Solution

This study reports a comparison of simulation results based on a two-dimensional model with experimental measurements in which the microwave of the TE_{10} mode operating at a frequency of 2.45 GHz is employed. In order to obtain the electromagnetic field inside a rectangular waveguide, a finite-difference time-domain (FDTD) method is applied [12]. The heat transport equation is solved by the method of finite differences based on the notion of control volumes [13]. Considering the microwave melting in the TE_{10} mode, it is the lowest mode of

TABLE I
THERMAL AND DIELECTRIC PROPERTIES OF LIQUID WATER AND ICE

Properties	Liquid water	Ice
ρ	1000 kg/m^3	1910.9 kg/m^3
λ	0.610 W/mK	1.48 W/mK
C_p	4.186 kJ/kgK	1.280 kJ/kgK
μ_r	1.0 H/m	1.0 H/m
ε_r	$88.15 - 0.414T + (0.131\times10^{-2})T^2 - (0.046\times10^{-4})T^3$	5.1 F/m
$\tan\delta$	$0.323 - (9.499\times10^{-3})T + (1.27\times10^{-4})T^2 - (6.13\times10^{-7})T^3$	0.0124

the supported microwave field for waves transmitted in the current rectangular waveguide without power dissipation. The type of wave mode is prescribed by the frequency and waveguide dimensions. Therefore, the calculated values of the wavelength of radiation in free space (λ) and the wavelength of radiation in rectangular waveguide (λ_g) are obtained as 122 and 148 mm, respectively. The wavelength of radiation in the layered packed beds ($\lambda_{\rm mg}$) can be calculated as a function of dielectric properties of the various components of the packed bed. Furthermore, the dielectric properties of the components depend on the temperature on the basis of the empirical relations of [8].

The computational domain is conservatively set such that the spatial resolution of each cell is $\Delta x = \Delta z \leq \lambda_{\rm mg}/10\sqrt{\varepsilon_r} \approx 1.0$ mm, thus, the total 112×605 cells in the computational domain were used in the numerical calculation. The temporal resolution is determined by $\Delta t \leq \sqrt{\Delta x^2 + \Delta z^2}/v \approx 1.0 \times 10^{-12}$ s, which satisfies the stability criterion.

It should be noted that the time step for the heat transfer is of the order of 1 s, which is very large compared with the time step required for the propagating velocity of waves. Some of electromagnetic and thermo-physical properties used in the numerical calculation are given in Table I. In addition, the detail of computational schemes and strategy are illustrated in Fig. 3.

IV. RESULTS AND DISCUSSIONS

Fig. 4(a) shows the experimental apparatus for the microwave melting system. The rectangular waveguide system shown in Fig. 4(b) operates by propagating traveling waves along the z-direction of the rectangular waveguide with inside dimensions of 109.22 mm $\times$ 54.61 mm toward a water load that is situated at the end of the waveguide. The water load (lower absorbing boundary) ensures that only a minimal amount of microwave is reflected back to the sample. Also, an isolator (upper absorbing boundary), which is located at the end of waveguide, is used to trap any microwaves reflected from the sample to prevent it from damaging the magnetron.

As shown in Fig. 4(c), the layered packed beds (dielectric material) considered are a packed beds of glass beads in either water or ice, which are then modeled as homogeneous and isotropic structures. These materials are selected to demonstrate the model because most of its physical properties are well documented. The unfrozen layer (glass beads and liquid water) with a thickness of 50 mm and the frozen layer (glass beads and ice) with a thickness of 50 mm are arranged in series perpendicular

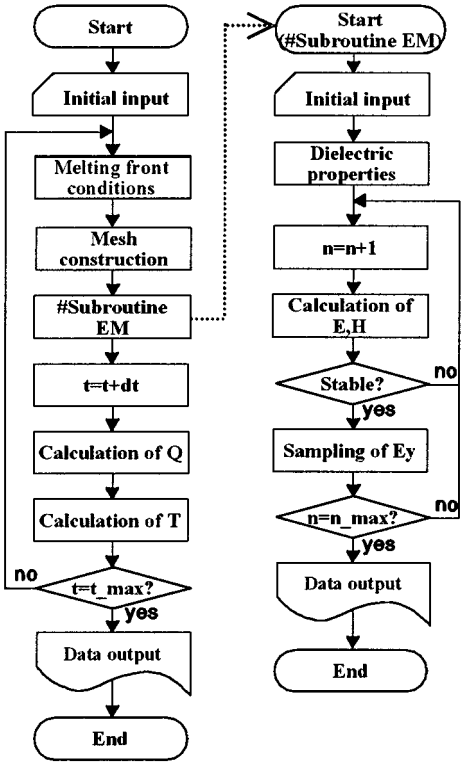

Fig. 3. Computational schemes.

to the direction of irradiation via a rectangular waveguide. The output of the magnetron is adjusted as 1000 W.

During the experiment, the microwave field was generated using a magnetron (model UM-1500, Micro Denshi Corporation, Tokyo, Japan). The powers of incident, reflected, and transmitted waves are measured by a wattmeter using a directional coupler (model DR-5000, Micro Denshi Corporation).

Figs. 5–8 show the simulation of temperature distribution and microwave energy absorbed within the layered packed beds in the vertical plane (x-z) in the cases setting the frozen layer on and under the unfrozen layer, respectively, which correspond to the initial temperature with 0 °C and microwave power level of 1000 W.

In the case of setting a frozen layer on the unfrozen layer (Figs. 5 and 7), the total microwave energy absorbed by the layered packed bed can increase because the microwaves are able to penetrate further into the packed bed. Moreover, setting of a frozen layer on the unfrozen layer protects the reflection of wave from the surface. The latter arises from the fact that the reflection and transmission components at each interface will contribute to the standing-wave pattern. Such pattern can lead to a much higher rate of microwave energy absorbed in the interior (Fig. 7). The presence of the strength of microwave energy absorbed gives rise to the hot spot in the leading edge of unfrozen layer. This causes heat to conduct from the hotter region in the unfrozen layer (higher microwave energy absorbed) to the cooler region (lower microwave energy absorbed) in the frozen layer. Consequently, the movement of the melting front occurs at the interface between the frozen and unfrozen layers.

In a continued melting process, the melting of the frozen layer is progressed where the strength of the microwave energy

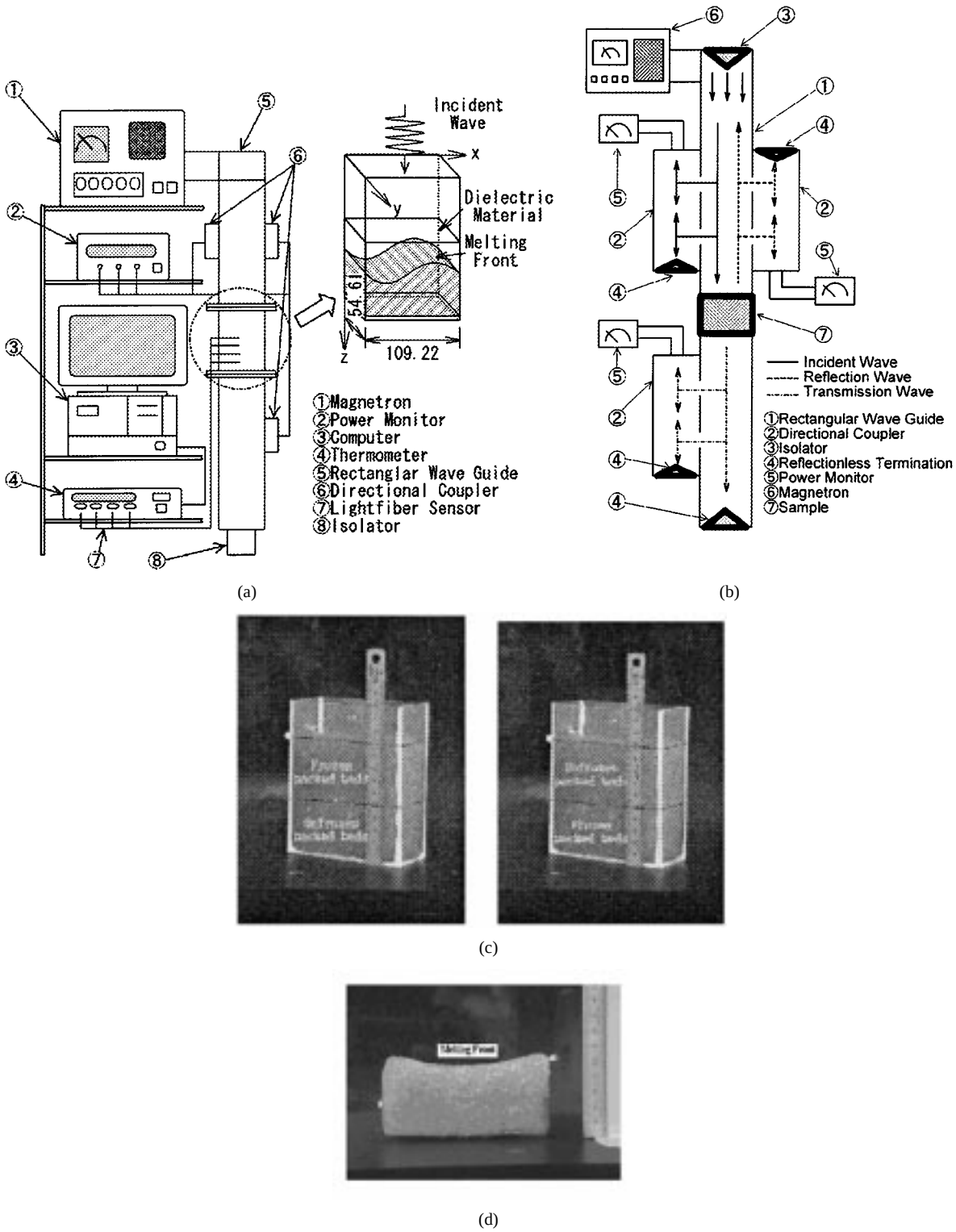

Fig. 4. Schematic of experimental facility. (a) Equipment setup. (b) Microwave measuring system. (c) Layered packed beds before melting. (d) Frozen packed bed after melting (setting a frozen layer on the unfrozen layer: 60 s).

absorbed increases (Fig. 7). Corresponding to that of the microwave energy absorbed, the temperature distribution within the unfrozen layer rapidly rises (Fig. 5) and decays slowly along the propagation direction because stronger standing waves form in the unfrozen layer. However, the temperature distribution within the frozen layer stays colder due to the difference between the dielectric properties of water and ice. This is because the water is a highly absorptive material, while ice is highly transparent (which corresponds to the lower microwave energy absorbed within frozen layer). At a time of 90 s, there is a difference of approximately 92° between the maximum and minimum temperatures.

In the case of setting a frozen layer under the unfrozen layer (Figs. 6 and 8), since the incident wave passing through the

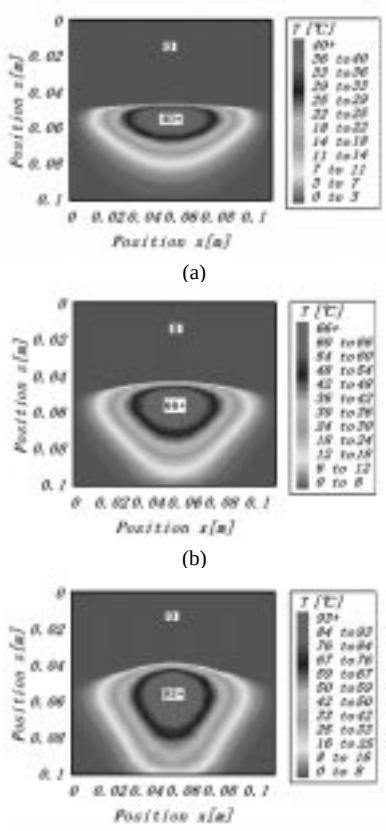

Fig. 5. Simulation of T at various times (setting a frozen layer on the unfrozen layer).

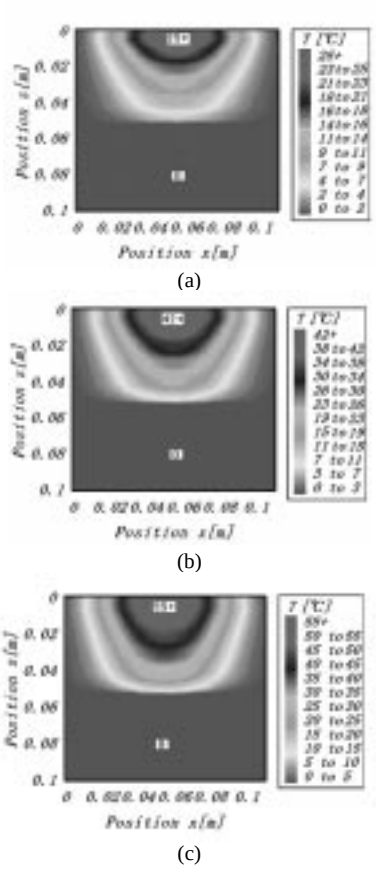

Fig. 6. Simulation of T at various times (setting a frozen layer under the upward unfrozen layer).

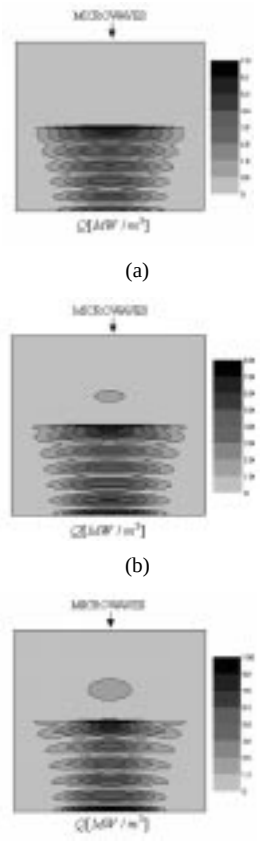

Fig. 7. Simulation of Q at various times (setting a frozen layer on the unfrozen layer).

cavity having a lower loss tangent coefficient is directly irradiated to the unfrozen layer having a higher loss tangent coefficient, the skin-depth heating effect causes a major part of the incident wave to be reflected from the surface. In additiona, having a frozen layer under the unfrozen layer protects the reflection of the microwave from the interface between the unfrozen and frozen layers. Consequently, the stronger standing wave does not form inside the layered packed beds, resulting in the strength of the microwave energy absorbed decreases (Fig. 8). This phenomenon explains why the magnitude of microwave energy absorbed in this case is slightly lower than that observed in the former case, and why the heating is more intensely close to the leading edge of the unfrozen layer (Fig. 6).

Furthermore, the distribution of temperature (Fig. 6) and microwave energy absorbed (Fig. 8) within the unfrozen layer slowly rise with the elapsed time corresponding to the microwave energy absorbed. Nevertheless, the distribution of temperature and microwave energy absorbed within the frozen layer is almost the same to the former case, indicating the dielectric properties' dominated melting process.

At 90 s, there is a difference of approximately 55° between the maximum and minimum temperatures. In contrast to that in the former case, in this case, the melting rate slowly rises with the elapsed time.

The following discussion refers to the effect of dielectric properties on the melting front during the microwave melting process. Fig. 9(a) and (b) shows the measured and predicted

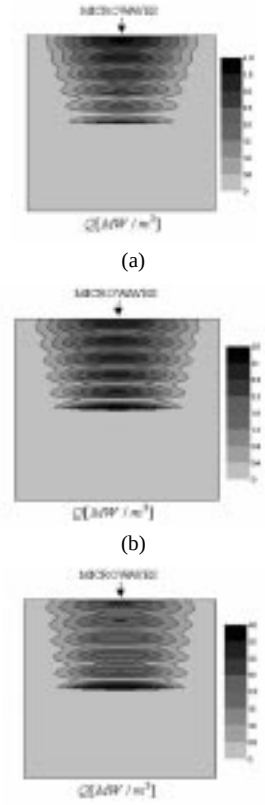

(a)

(b)

(c)

Fig. 8. Simulation of Q at various times (setting a frozen layer under the unfrozen layer).

results of the melting front in the cases of setting a frozen layer on and under the unfrozen layer, respectively.

In the former case [see Fig. 9(a)], the shapes of the melting front at various times are shown in Fig. 9(a). It is seen that most of the heating occurred at the center of the rectangular waveguide where the microwave energy absorbed is maximum. The central region of the frozen layer rapidly shows the signs of melting while the outer edge displays no obvious sign of melting, indicating that the temperature did not exceed 0 °C [as referred in Fig. 4(d)].

However, in the early stages of the melting process, the melting front is almost parallel to the interface between the frozen and unfrozen layers. Later, the melting front gradually exhibits a shape typical for heat conduction dominated melting.

In the latter case [see Fig. 9(b)], in contrast to that in former case, the melting front slowly moves with the elapsed time along the propagation direction due to the characteristics of dielectric properties, as explained in Figs. 6 and 8.

The observation of the melting front depicted in Fig. 9(a) and (b) for the layered packed beds verifies that the match between the simulation results and experimental data is good, with the simulation results exhibiting the same overall trend of the experimental profiles. However, at longer melting times (90 s), the experimental data are significantly higher than that simulation results. The source of the discrepancy is the nonuniform heating effect along the axis, which accounts for the fact that the incident microwave at the surface of layered packed beds is nonuniform. Numerically, the discrepancy may be attributed to uncertainties in the thermal and dielectric property database.

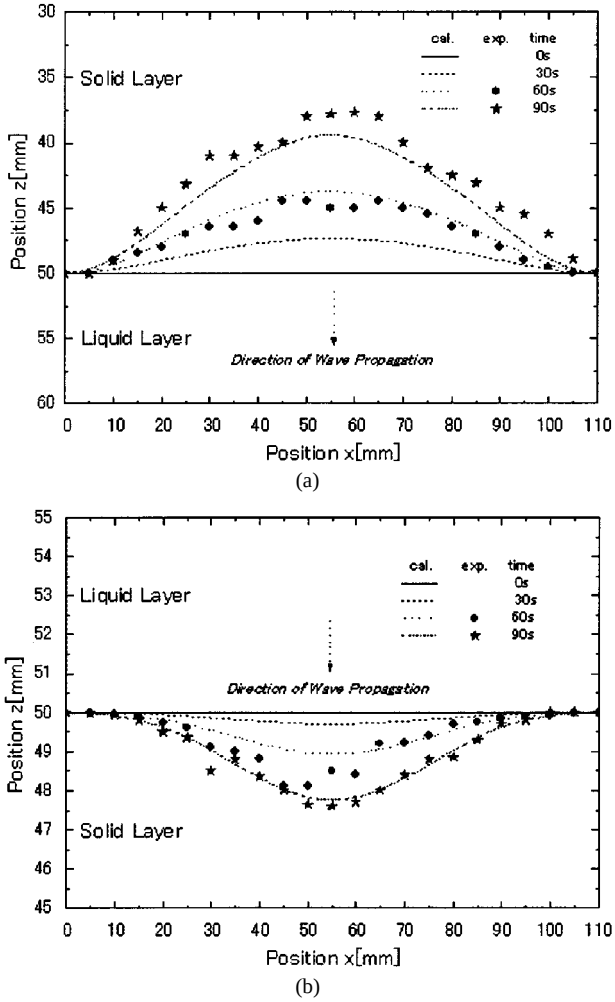

(a)

(b)

Fig. 9. Measured and predicted interface position. (a) Setting a frozen layer (solid) on the unfrozen layer (liquid). (b) Setting a frozen layer (solid) under the unfrozen layer (liquid).

Furthermore, during the experiment of the microwave melting process, the impact on the uncertainty of our data may cause variations in humidity, room temperature, and another effects. The uncertainty in melting kinetics was assumed to result from errors in the measured melting front of the layered packed beds. The calculated melting kinetic uncertainties in all tests were less than 3.5%. The uncertainly in microwave energy absorbed was assumed to result from errors in measured input power and reflected power. The calculated uncertainty associated with microwave power was less than 2%.

From this study, the capability of the mathematical model to correctly handle the field variations at the interfaces between materials of different dielectric properties is shown. With further quantitative validation of the mathematical model, it is clear that the model can be used as a real tool for investigating in detail this particular microwave heating of dielectric materials at a fundamental level.

V. Conclusion

The following results concerning the microwave melting phenomena have been obtained.

1) A generalized mathematical model of the melting process by a microwave has been proposed and success-

fully used to describe the melting phenomenon of several conditions.

2) The result has shown that the changing of the established position of layered packed beds changes the degree of the penetrated microwave and the rate of microwave energy absorbed within the layered packed beds. Setting a frozen layer (solid) on the unfrozen layer (liquid), the reflection and transmission components at each interface will contribute to the standing-wave pattern. Such a pattern can lead to a much higher melting rate in the interior.
3) Also, the direction of melting against the incident microwave strongly depends on that established position of layered packed beds. This is because of the difference in the dielectric properties between water and ice within layered packed beds.
4) The reflection rate of microwave in layered packed beds strongly depends on the dielectric properties of melting materials.
5) Based on a model combined with the electromagnetic and temperature fields, the predicted results were in good agreement with the experimental results for the melting of frozen packed beds.

REFERENCES

[1] B. J. Pangrle and K. G. Ayappa, "Microwave thawing of cylinders," *AIChE J.*, vol. 37, pp. 1789–1800, 1991.
[2] X. Zeng and A. Faghri, "Experimental and numerical study of microwave thawing heat transfer for food materials," *ASME J. Heat Transfer*, vol. 116, pp. 446–455, 1994.
[3] T. Basak and K. G. Ayappa, "Analysis of microwave thawing of slab with the effective heat capacity method," *AIChE J.*, vol. 43, pp. 1662–1674, 1997.
[4] F. Torres and B. Jecko, "Complete FDTD analysis of microwave heating process in frequency-dependent and temperature dependent media," *IEEE Trans. Microwave Theory Tech.*, vol. 45, pp. 108–117, Jan. 1997.
[5] L. Feher, G. Link, and M. Thumm, "The MiRa/THESIS-code package for resonator design and modeling of millimeter-wave material processing," in *Proc. Mater. Res. Soc. Spring Meeting Symp.*, vol. 430, San Francisco, CA, 1996, pp. 363–368.
[6] P. Ratanadecho, K. Aoki, and M. Akahori, "Influence of irradiation time, particle sizes, and initial moisture contents during microwave drying of multi-layered capillary porous materials," *ASME J. Heat Transf.*, vol. 124, pp. 151–161, 2002.
[7] K. Aoki, P. Ratanadecho, and M. Akahori, "Characteristics of microwave heating for multi-layered materials using a rectangular wave guide," in *Proc. 4th JSME–KSME Thermal Eng. Conf.*, vol. 2, Kobe, Japan, Oct. 1–6, 2000, pp. 191–196.
[8] P. Ratanadecho, K. Aoki, and M. Akahori, "A numerical and experimental study of microwave drying using a rectangular wave guide," *Drying Technol. J.*, vol. 19, no. 9, pp. 2209–2234, 2001.
[9] A. R. Von Hippel, *Dielectric Materials and Applications*. Cambridge, MA: MIT Press, 1954.
[10] G. Mur, "Absorbing boundary conditions for the finite-difference approximation of the time-domain electromagnetic-field equations," *IEEE Trans. Electromagn. Compat.*, vol. EMC-23, no. 4, pp. 377–382, 1981.
[11] L. E. Eriksson, "Generation of boundary-conforming grid around wing-body configurations using transfinite interpolation," *AIAA J.*, vol. 20, pp. 1313–1320, 1982.
[12] S. Tada, R. Echigo, Y. Kuno, and H. Yoshida, "Numerical analysis of electromagnetic wave in partially loaded microwave applicator," *Int. J. Heat Mass Transf.*, vol. 41, pp. 709–718, 1998.
[13] S. V. Patankar, *Numerical Heat Transfer and Fluid Flow*. Bristol, PA: Hemisphere, 1980.

Phadungsak Ratanadecho was born in Thailand, on July 12, 1968. He received the B.Eng. degree in mechanical engineering from the King Mongkut University of Technology Thonburi, Bangkok, Thailand, in 1991, the M.Eng. degree in mechanical engineering from Chulalongkorn University, Bangkok, Thailand, in 1994, and the Ph.D. degree in the mechanical engineering from the Nagaoka University of Technology, Nagaoka, Japan, in 2002.

From 1991 to 1992, he was with The Shell Company, Bangkok, Thailand, where he was a Mechanical Engineer. From 1994 to 1997, he was a Section Manager with The Aromatics Corporation, Rayong, Thailand. Since 1997, he has been a Lecturer in the Department of Mechanical Engineering, Thammasat University, Pathumthani, Thailand. His main research interests include the computational and experimental study of heat and fluid flow in porous medium, microwave heating, and microwave drying in porous medium.

Dr. Ratanadecho was the recipient of a 1998–2002 Japanese Government Scholarship (Monbucho).

Kazuo Aoki was born in Toyama, Japan, on March 3, 1951. He received the Ph.D. degree in mechanical engineering from the Tokyo Institute of Technology, Tokyo, Japan, in 1978.

From 1978 to 1994, he was with the Department of Mechanical Engineering, Nagaoka University of Technology, Japan, where he was a Research Associate (1978–1979), an Assistant Professor (1980–1981), and an Associate Professor (1981–1994). He is currently a Professor in the Department of Mechanical Engineering, Nagaoka University of Technology, Niigata, Japan. His current research interests are freezing and melting processes in porous medium, molecular dynamics in heat and mass transfer, and the applications of microwave processing in engineering fields.

Dr. Aoki was conference chair for several conferences held in Japan.

Masatoshi Akahori was born in Toyama, Japan. He received the Ph.D. degree in mechanical engineering from the Nagaoka University of Technology, Niigata, Japan, in 1998.

He is currently a Research Associate in the Department of Mechanical Engineering, Nagaoka University of Technology. His research interests include freezing and melting processes in porous medium and microwave drying of capillary porous medium.